

# X-ray photoelectron spectroscopy studies of polycrystalline samples $\text{NbB}_{2+x}$

R. Escamilla and L. Huerta

Instituto de Investigaciones en Materiales. Universidad Nacional Autónoma de México.

04510 México D.F., México.

## ABSTRACT

Polycrystalline samples with nominal composition  $(\text{B}/\text{Nb}) = 2.0, 2.1, 2.2, 2.3, 2.4$  and  $2.5$  were studied by X-ray photoelectron spectroscopy (XPS). The spectra revealed Nb and B oxides on the surface of the samples, mainly  $\text{B}_2\text{O}_3$  and  $\text{Nb}_2\text{O}_5$ . After long periods of etching time the intensity of Nb and B oxides decreased. The Nb  $3d_{5/2}$  and B 1s core levels associated with the chemical states  $(\text{B}/\text{Nb})$  were identified and they do not change with etching time. The Binding Energy (BE) of the Nb  $3d_{5/2}$  and B 1s core levels increase as boron content increases, suggesting a positive chemical shift in the core levels. On the other hand, analysis of Valence Band spectra show that the contribution of the Nb  $4d$  states slightly decreases while the contribution of the B  $2p_\pi$  states increases with the increase of boron content. As a consequence, the electronic and superconducting properties are modified substantially, in agreement with band-structure calculations.

**Keywords:** Polycrystalline Niobium diboride; X-ray photoelectron spectroscopy; band structure

**PACS:** 74.25.Jb; 79.60. - I; 82.80.Pv

## 1. INTRODUCTION

Since the discovery of superconductivity in  $\text{MgB}_2$  with a transition temperature  $T_c$  of 39 K [1] much experimental [2-5] and theoretical [6-8] research has been carried out on this compound and on a series of isostructural diborides. Band structure calculations in  $\text{MgB}_2$  clearly reveal that while strong covalent B-B bond is retained within boron planes, the Mg-B bond is ionic and the two electrons of Mg are fully donated to the B [9]. On the other hand, studies on the bond ionicity in the  $4d$  transition metals diborides have shown that the factor of ionicity ( $f_i$ ) of Me-B bond (Me = transition metals) decreases with the decrease of the atomic number ( $Z$ ) of the metal [10]. In the case of  $\text{MgB}_2$ , the Mg-B bond has the largest  $f_i$ . Apparently, the existence of delocalization of valence electrons between layers

and various types of bonds induces changes in the stoichiometry and modifies the electronic properties in these compounds [11]. Most non-stoichiometric compounds appear by decreasing of *fi* in 4*d* transition metals diborides. An example is the niobium diboride [12-14]. In spite of the fact that the electronic properties of transition metal diborides have been well studies, details of the electronic structure of non-stoichiometric NbB<sub>2</sub> compound are a matter of debate in the literature [15, 16]. Moreover, there is no consensus as the character of the chemical bond is involved. Some researchers believe that the boron atoms behave as donors [17-19] while in others argue that charge transfer is in the opposite direction [20-22]. X-ray photoelectron spectroscopy (XPS) is one of the most effective and direct methods of investigating the type of chemical bond in molecules and crystalline solid. This paper show the importance of non-stoichiometry in the electronic and superconducting properties of NbB<sub>2</sub> and it is determined the chemical state of the boron and niobium atoms.

## 2. EXPERIMENTAL

We synthesized samples with nominal composition (B/Nb) = 2.0, 2.1, 2.2, 2.3, 2.4 and 2.5 by the solid-state reaction method. The precursors, commercially available NbB<sub>2</sub> powder (Aldrich, -325 mesh) and boron (99.5 % powder, crystalline, < 57 mesh, 99.5 mass %) were mixed in stoichiometric amounts and pressed into pellets with 6 mm in diameter and 0.6–1 g in weight. The pellets were placed in stainless steel sealed tubes. The samples were sintered in a tube furnace at 1000 °C for 3 h in Ar atmosphere and quenched to room temperature. Phase identification of the samples was done with an X-ray diffractometer (XRD) Siemens D5000 using Cu-K<sub>α</sub> radiation and a Ni filter. Intensities were measured in steps of 0.02° for 14 seconds in the 2θ range 10° – 110° at room temperature. Crystallographic parameters were refined using the program Quanto (A Rietveld program

for quantitative phase analysis of polycrystalline mixtures) with multi-phase capability [23]. The chemical analysis was carried out by X-Ray Photoelectron Spectroscopy (XPS). This analysis was performed using an UHV system of VG Microtech ESCA2000 Multilab, with an Mg K<sub>α</sub> X-ray source ( $h\nu = 1253.6$  eV), operated a 15kV and 20 mA beam, and CLAM4 MCD analyser. The surface of the pellets was etched during 5 minutes with 4.5kV Ar<sup>+</sup> at 4 $\mu$ A in 12 mm<sup>2</sup>. The XPS spectrum was obtained at 55° of the normal surface in the constant pass energy mode,  $E_0=50$ eV and 20eV for survey and high resolution narrow scan. The atomic relative sensitivity factor (RSF) reported by Scofield was corrected by transmission function of the analyzer [24] and by reference material Nb<sub>2</sub>O<sub>5</sub>, B, Nb and B<sub>2</sub>O<sub>3</sub>. The peak positions were referenced to the background silver 3d<sub>5/2</sub> photopeak at 368 eV. The FWHM is 1.0 eV for referent to the Ag 3d<sub>5/2</sub>, and C 1s hydrocarbon groups in 284.5 eV central peak position. The XPS spectra were fitted with the program SDP v 4.1 [25]. The XPS error is based considering a detection limit estimated to be ~0.1 % and uncertain propagation. The uncertain associated to the atomic composition calculated is 3% due to the maximum deviation of the reference materials B<sub>2</sub>O<sub>3</sub> and Nb<sub>2</sub>O<sub>5</sub>.

### 3. RESULTS AND DISCUSSION

Fig. 1 shows the powder X-ray diffraction (XRD) patterns obtained for the nominal compositions (B/Nb) = 2.0, 2.1, 2.2, 2.3, 2.4 and 2.5. The main features correspond to the NbB<sub>2</sub> phase (ICDD n° 75-1048). The authors have shown previously [26] that a) the NbB<sub>2</sub> phase is the most abundant in all samples studied > 94%, b) by Rietveld method the real compositions denominated (B/Nb)<sub>ref</sub> were calculated from the nominal compositions (B/Nb) and c) from these results we have discussed that not all of the excess of boron is incorporated in the NbB<sub>2</sub> phase, and finally we demonstrated that the boron in excess into the structure is accompanied by the creation of vacancies on the metal (Nb) site, producing

important changes in the electronic and superconducting properties. Recently, C. A. Nunez et al [27] obtained similar results by studies of neutron diffraction in  $\text{NbB}_{2+x}$  samples.

In order to examine the stoichiometry as well as the formation of some other phases, we analyzed the polycrystalline samples by X-ray photoelectron spectroscopy (XPS). Fig. 2 shows the XPS spectra before (a) and after (b) etching for polycrystalline samples with nominal compositions  $(\text{B}/\text{Nb}) = 2.0, 2.1, 2.2, 2.3, 2.4$  and  $2.5$ . It is observed that the surface of the polycrystalline samples before etching, exhibits significant levels of C, N and O in addition to Nb and B oxides. For more clarity, in the Figs. 3 a) and 3 b) the deconvoluted XPS spectra of the Nb  $3d_{5/2}$  band before and after etching for the composition  $(\text{B}/\text{Nb}) = 2.0$  are shown. In the process of fitting of the Nb 3d XPS spectra we fixed the values of Binding Energy (BE) for  $\text{Nb}^{5+}3d_{5/2}$ ,  $\text{Nb}^{4+}3d_{5/2}$  and  $\text{Nb}^{2+}3d_{5/2}$  core levels at: 207.57 eV, 206.10 eV and 204.70 eV, respectively. Before etching, the surface of sample shows that the  $\text{Nb}^{5+}3d_{5/2}$  core level associated to  $\text{Nb}_2\text{O}_5$ , which differs qualitatively from at after etching the surface. In the former case, the intensity of core level is higher than in the latter case (see Fig. 3 a). Different authors suggest that the presence of  $\text{Nb}_2\text{O}_5$  in the surface is due to the sample contact with the ambient atmosphere [28, 29]. In addition to the core level associated to  $\text{Nb}_2\text{O}_5$ , two pairs of core levels of poor intensity are identified. The first one is associated to  $\text{NbO}_2$  ( $\text{Nb}^{4+}3d_{5/2}$ ) and appears at BE = 1.47 eV lower than that of  $\text{Nb}_2\text{O}_5$ . The second is associated to  $\text{NbO}$  ( $\text{Nb}^{2+}3d_{5/2}$ ) and appears at BE = 2.3 eV above that of the Nb metal (BE = 202.40 eV), which is 0.4 eV on average below the value previously reported [30].

After etching, the intensity of C 1s (BE = 284.50 eV), N 1s (BE = 400 eV) and O 1s (BE = 532.00 eV) core levels diminishes, in the same way that  $\text{Nb}_2\text{O}_5$ . Meanwhile, the intensity of core levels associated with  $\text{NbO}$  and  $\text{NbO}_2$  increases as it can be seen in the

Figs. 2 b) and 3 b) [31]. In particular, we observed that the intensity of NbO core levels is higher than that associated to NbO<sub>2</sub>. Fig.4 shows the effect of etching time on the core levels for the composition (B/Nb) = 2.0. It is observed the appearance of a structure on the lower BE side of the Nb 3d<sub>5/2</sub> core level at BE= 203.34 eV with the increase of etching time. Comparing this with the reference Nb metallic core level we observed a chemical shift of 0.94 eV. As we can see, for etching time longer than 5 min there is no any further change in the Nb 3d<sub>5/2</sub> core level unlike the Nb oxides, implying that the stoichmetry of the (B/Nb) = 2.0 to 2.5 samples remain stable.

In order to determine the real compositions of the samples studied, the atomic compositions were calculated by XPS using the survey spectra with RSF of Nb 3d and B 1s. As it can be observed, the calculated compositions by XPS are very close to the compositions calculated by Rietveld refinement [26] (see Table 1).

Fig. 5 a) shows the deconvolution of XPS spectra in the Nb 3d region for the compositions (B/Nb)<sub>XPS</sub> = 2.00(6) to 2.44(8) after etching. These XPS spectra fitted shows an increase of the BE of the Nb 3d<sub>5/2</sub> core level in the range 2.00(6) ≤ (B/Nb)<sub>XPS</sub> ≤ 2.27(7) and a slight decrease for the range 2.41(7) ≤ (B/Nb)<sub>XPS</sub> ≤ 2.44(8). As a consequence, we observed a positive chemical shift in the Nb 3d<sub>5/2</sub> core level. Similar positive chemical shift are observed in the 3d transition metal borides respect to metals [32].

Fig. 5 b) shows the deconvolution of XPS spectra in the B 1s region for the compositions already mentioned after etching. The B 1s core level associated with the composition (B/Nb)<sub>XPS</sub> = 2.00(6) is localized at BE = 188.15 eV, this value is within the binding energy variation range for typical transition metal diborides (187.1–188.3 eV [33, 34]) and borocarbides RNi<sub>2</sub>B<sub>2</sub>C (R =Y and La) [35]. This observation is qualitatively consistent with reported calculations and maximum entropy method (MEM) results, shown that B – B

bonding is two-dimensionally covalent ( $sp^2$ ) [6, 36-38]. In addition, core levels at BE = 193.10 eV, 195.10 eV and 197.67 eV have been observed, the first one correspond to  $B_2O_3$  while the rest are associated to satellites of Nb due to the x ray source (Mg  $K_\alpha$ ) and not to satellite shake-up of boron compounds [39]. Furthermore, it is clearly observed an increase of the BE of B 1s core level in the range  $2.00(6) \leq (B/Nb)_{XPS} \leq 2.27(7)$  and remain constant for greater concentrations (see table 1). The maxima positive chemical shift (0.90 eV) correspond to the compositions  $(B/Nb)_{XPS} = 2.27(7)$ ,  $2.41(7)$  and  $2.44(8)$ .

In comparison, in the 3d transition metal borides the BE of B1s is lower than that in pure boron and the BE of transition metal  $Me\ 2p_{3/2}$  ( $Me = 3d$  transition metal) is higher than that of the metal. In other words, a negative chemical shift for B1s and a positive chemical shift for  $Me\ 2p_{3/2}$  core level are observed [32]. It is important to point out that the chemical shifts in BE are often used to study the electronic redistribution or charge transfer upon compound and alloying.

In a conventional XPS interpretation, the general rule is that the BE of the central atom increases as the electronegativity of the attached atoms or groups increases [40]. Since B (2.04) is more electronegative than Nb (1.6) according to Pauling's electronegativity table [41], one would expect that the B core level shift toward the lower binding energy. For example, in the  $TiB_2$ , the BE of B1s is lower than in pure boron and the BE of  $Ti\ 2p_{3/2}$  is higher than Ti metal, in this case the authors assume that some charge transfer occur from the Ti atoms to the boron atoms. This observation is confirmed by results obtained by the discrete-variational  $X\alpha$  method [42]. The magnitude of this electron donation decreases from  $ScB_2$  to  $FeB_2$  [43]. Thus, the high donor ability of scandium and the slightly smaller donor ability of titanium in the diborides are corroborated by the fact that the BE of the B 1s in  $TiB_2$  is greater than that in  $ScB_2$  and even smaller than that in pure boron.

Furthermore, the studies of XPS in  $\text{MgB}_2$  shown that the BE of B1s is lower than that in pure boron [44, 45] and the BE of Mg 2p is higher than that in Mg metal [45], then on the basis of previous experimental facts it is possible to speculate that some charge transfer occurs from the Mg atoms to the boron atoms. Studies of Valence-electron distribution in  $\text{MgB}_2$  by accurate diffraction measurements and first-principles calculations confirm this observation [46]. From Table 1, it is clear that the general rule based on the electronegativity table fails to explain the positive chemical shift in B 1s core level of our samples studied. Therefore the presence of superconductivity in these samples does not can be explained by a charge transfer model based only on chemical shift effects.

In order to determine the effect of boron excess on the density of states at the Fermi level  $N(E_F)$ , we measured the Valence Band using a monochromatic Al K $\alpha$  source. Fig. 6 shows the normalized Valence Band spectra for the compositions  $(\text{B}/\text{Nb})_{\text{XPS}} = 2.00(6)$  and  $(\text{B}/\text{Nb})_{\text{XPS}} = 2.44(8)$ . The discontinuous lines delimit the niobium and boron states respect to  $N(E_F)$ . The total density of states (DOS) for  $\text{NbB}_2$  determined from band-structure calculations [15, 47] is shown below the measured spectrum, a good correspondence with the measured spectrum is obtained if the DOS is shifted to higher binding energy by 4 eV, as shown in Fig. 6. Similar shifts of  $\sim 2$  eV are required for high-temperature superconductors, and have been attributed to electron correlation effects. In particular, comparing with band-structure calculations the feature between 8 and 12 eV is due to the B 2s states observed also in  $\text{MgB}_2$  [7,9, 49,50] while that the feature at 5–8 eV is due to predominantly B 2p $_{\pi}$  states [48] to difference of the B 2p $_{\sigma}$  states that contribute in  $\text{MgB}_2$  at  $N(E_F)$  [9, 11]. On the other hand, the feature around 2 eV is associated to the Nb 4d states [15]. Because the main contribution to  $N(E_F)$  of  $\text{NbB}_2$  are the Nb 4d states, the  $N(E_F)$  of this

phase is greater than that for  $\text{MgB}_2$ , the former is 1.074 states/eV-cell while that for the latter is 0.719 states/eV-cell [47].

Comparing both Valence Band spectra, we observed that for  $(\text{B/Nb})_{\text{XPS}} = 2.44(8)$ , the density of states at the Fermi level  $N(E_F)$  decreases only slightly due to a decrease in the contribution  $N^{\text{Nb}}(E_F)$  of the Nb  $4d$  states, whereas the contribution  $N^{\text{B}}(E_F)$  of the B  $2p_{\pi}$  states increases, respect to  $(\text{B/Nb})_{\text{XPS}} = 2.00(6)$ . Therefore, the changes observed in the density of states at the Fermi level  $N(E_F)$  due mainly to the contribution of B  $2p_{\pi}$  states can contribute to increase the superconducting carrier density.

This result is supported by muon spin rotation/relaxation measurements in  $\text{NbB}_{2+x}$  samples [51]. The authors suggest that the superconducting order parameter in  $\text{NbB}_{2+x}$  is isotropic, as expected for conventional BCS superconductors. Meanwhile, the superconducting carrier density ( $\propto \lambda^2$ ) exhibits an interesting tendency of increase with increasing  $T_c$  (where  $T_c$  varies with  $x$ ), which is described by the weak-coupling BCS theory.

#### 4. CONCLUSIONS

We have prepared samples with nominal composition  $(\text{B/Nb}) = 2.0 - 2.5$  by the solid-state reaction method. The real compositions were calculated from nominal composition by XPS. Our XPS results indicate that the compositions change from  $(\text{B/Nb})_{\text{XPS}} = 2.00(6) - 2.44(8)$ . The stoichiometry of these compositions is stable during large periods of etching time. Particularly, we distinguish that the Nb  $3d_{5/2}$  and B 1s core levels are associated to the chemical states of the composition  $(\text{B/Nb})_{\text{XPS}}$ . For  $(\text{B/Nb})_{\text{XPS}} = 2.00(6)$ , the Nb  $3d_{5/2}$  and B 1s core levels are localized at 203.34 eV and 188.15 eV, respectively. As a consequence of the increase in the boron content, a positive chemical shift is observed in the Nb  $3d_{5/2}$  and B 1s core levels. For the compositions  $(\text{B/Nb})_{\text{XPS}} \geq 2.27(7)$  we observed the maximum positive chemical shifts in the Nb  $3d_{5/2}$  and B 1s core levels. The study of the Valence Band

for  $\text{NbB}_2$  phase is consistent with band-structure calculations, we results shown a slight decrease in the contribution of the Nb  $4d$  states and an increase in the contribution of the B  $2p_\pi$  states to the density of states at the Fermi level  $N(E_F)$  with the increase of boron content. Finally, although we cannot apply the charge transfer model based on concepts of electronegativity in our study; we could associate the maximum  $T_c$  (9.40 - 9.75 K) previously reported with the increase the superconducting carrier density due at the increasing in the contribution B  $2p_\pi$  at density of states at the Fermi level  $N(E_F)$ .

## ACKNOWLEDGEMENTS

Support from DGAPA-UNAM under project PAPIIT-IX101104 and PAPIIT IN105404 is gratefully acknowledged. Thanks to A. Durán and J. C. Alonso for carefully reading and correcting the manuscript.

## REFERENCES

- [1] J. Nagamatsu, N. Nakagawa, T. Muranaka, Y. Zenitani, J. Akimitsu, *Nature* (London) **410**, 63 (2001).
- [2] E. Z. Kurmaev, I. I. Lyakhovskaya, J. Kortus, A. Moewes, N. Miyata, M. Demeter, M. Neumann, M. Yanagihara, M. Watanabe, T. Muranaka, and J. Akimitsu, *Phys. Rev. B* **65**, 134509 (2002).
- [3] T. A. Callcott, L. Lin, G. T. Woods, G. P. Zhang, J. R. Thompson, M. Paranthaman and D. L. Edererm. *Phys. Rev. B* **64**, 132504 (2001).
- [4] S. L. Bud'ko, G. Lapertot, C. Petrovic, C. E. Cunningham, N. Anderson, and P. C. Canfield, *Phys. Rev. Lett.* **86**, 1877 (2001).
- [5] Herbert Schmidt, J. F. Zasadzinski, K. E. Gray, and D. G. Hinks, *Phys. Rev. B* **63**, 220504 (2001).

[6] Kortus J, Mazin I I, Belashchenko K D, Antropov V P and Boyer L L *Phys. Rev. Lett.* **86**, 4656 (2001).

[7] K. D. Belashchenko, M. van Schilfgaarde, and V. P. Antropov, *Phys. Rev. B* **64**, 092503 (2001).

[8] G. Satta, G. Profeta, F. Bernardini, A. Continenza, and S. Massidda, *Phys. Rev. B* **64**, 104507 (2001).

[9] J.M. An and W. E. Pickett, *Phys. Rev. Lett.* **86**, 4366 (2001).

[10] L. Wu, M. He, L. Dai, X.L. Chen and Q. Y. Tu, *J. Phys: Cond. Matter* **13**, 723 (2001).

[11] I.I. Mazin, V.P. Antropov, *Physica C* **385**, 49 (2003).

[12] A.S. Cooper, E. Corenzwit, L.D. Longinotti, B.T. Matthias, W.H. Zachariasen, *Proc. Nat. Acad. Sci.* **67**, 313 (1970).

[13] J.E. Schriber, D.L. Overmeyer, B. Morosin, E.L. Venturini, R. Baughman, D. Emin, H. Klesnar, T. Aselage, *Phys. Rev. B* **45**, 10787 (1992).

[14] A. Yamamoto, C. Takao, T. Masui, M. Izumi, S. Tajima, *Physica C* **383**, 197 (2002).

[15] I. R. Shein, N. I. Medvedeva and A. L. Ivanovski, *Physics of the Solid State* **45**, 1541 (2003).

[16] P. J. Thomas Joseph and P. P. Singh, *Physica C* **391**, 125 (2003)

[17] H. J. Juretschke and R. Stinitz, *J. Phys. Chem. Solids* **4**, 118 (1957).

[18] R. Kiessling, *Acta Chem. Scand.* **4**, 209 (1957).

[19] M. C. Cadeville, *J. Chem. Solids* **27**, 667 (1966).

[20] W. N. Lipscomb and D. Britton, *J. Chem. Phys.* **33**, 275 (1957).

[21] L. Pauling, *Proc. R. Soc. London, Ser. A* **196**, 343 (1949).

[22] R. W. Johnson and A. H. Daane, *J. Chem. Phys.* **38**, 425 (1963).

[23] Altomare, A., Burla, M.C., Giacovazzo, C., Guagliardi, A., Moliterni, A.G.G., Polidori, G., Rizzi, R. *J.Appl.Cryst.* **34**, 392 (2001).

[24] J.H. Scofield, *Journal Electron Spectrosc.* **8**, 129 (1976).

[25] SDP v4.1 (32 bit) Copyright © 2004 , XPS International, LLC , Compiled January 17, 2004

[26] R Escamilla, O Lovera, T Akachi, A Duran, R Falconi, F Morales and R Escudero. *J. Phys.: Condens. Matter* **16**, 5979 (2004)

[27] C. A. Nunes, D. Kaczorowski, P. Rogl, M. R. Baldissera, P. A. Suzuki, G. C. Coelho, A. Grytsiv, G. Andre', F. Bouree', S. Okada, *Acta Materialia* **53** 3679 (2005)

[28] M. Grundner, J. Halbritter, *Surf. Sci.* **136**, 144 (1984)

[29] J. Halbritter, *Appl. Phys. A: Solids Surf.* **43**, 1 (1987).

[30] B. R. King, H. C. Patel, D. A. Gulino, B. J. Tatarchuk, *Thin Solid Films* **192**, 351 (1990)

[31] P. C. Karulkar. *J. Vac. Sci. Technol.* **18**, 169 (1981).

[32] V. G. Aleshin, T. Y. Kosolapova, V. V. Nemoshkalenko, T. I. Serebryakova and N. G. Chudinov. *Journal of the Less-Common Metals*, **67**, 173 (1979)

[33] G. Mavel, J. Escard, P. Costa, and J. Castaing, *Surf. Sci.* **35**, 109 (1973).

[34] C. L. Perkins, R. Singh, M. Trenary, T. Tanaka, and Y. Paderno, *Surf. Sci.* **470**, 215 (2001).

[35] K. Kobayashi, T. Mizokawa, K. Mamiya, A. Sekiyama, A. Fujimori, H. Takagi, H. Eisaki, S. Uchida, R.J. Cava, J.J. Krajewski, W.F. Peck Jr., *Phys. Rev. B* **54** 507 (1996).

[36] J.M. An, W.E. Pickett, *Phys. Rev. Lett.* **86** 4366 (2001).

[37] N.I. Medvedeva, A.L. Ivanovskii, J.E. Medvedeva, A.J. Freeman, *Phys. Rev. B* **64** 020502 (2001).

[38] E. Nishibori, M. Takata, M. Sakata, H. Tanaka, T. Muranaka, J. Akimitsu, *J. Phys. Soc. Jpn.* **70**, 2252 (2001).

[39] I. Jiménez, D. G. J. Sutherland, T. van Buuren, J. A. Carlisle, and L. J. Terminillo, *Phys. Rev. B* **57** 167 (1998).

[40] W.F. Egelhoff Jr., *Surf. Sci. Rep.* **6**, 253 (1987).

[41] L. Pauling, in: 3rd Edition, *The Nature of the Chemical Bond*, Cornell University Press, Ithaca, New York, 1957.

[42] M. Mizuno, I. Tanaka, and H. Adachi, *Phys. Rev. B* **59** (1999) 15033

[43] P. Vajeeston, P. Ravindran, C. Ravil and R. Asokamani1, *Phys. Rev. B* **63**, 045115 (2001)

[44] R.P. Vasquez, C.U. Jung, Min-Seok Park, Hoon-Jung Kim, J.Y. Kim and Sung-Ik Lee, *Phys. Rev. B* **64** 052510 (2001) .

[45] K.B. Garg, T. Chatterji, S. Dalela, M. Heinonen, J. Leiro, B. Dalela and R.K. Singhal, *Sol. St. Comm.* **131**, 343 (2004).

[46] Lijun Wu, Yimei Zhu, T. Vogt, Haibin Su, J. W. Davenport and J. Tafto. *Phys. Rev. B*. **69**, 064501 (2004)

[47] I. R. Shein, and A. L. Ivanovski, *Physics of the Solid State* **44**, 1833 (2002).

[48] J. Nakamura, N. Yamada, K. Kuroki, T. A. Callcott, D. L. Ederer, J. D. Denlinger, R. C. C. Perera, *Phys. Rev. B* **64**, 174504 (2001)

[49] H. Rosner, J.M. An, W.E. Pickett, and S.-L. Drechsler, *Phys. Rev. B* **66**, 024521 (2002).

[50] P.P. Singh, *Phys. Rev. Lett.* **87**, 087004 (2001).

[51] H. Takagiwa, S. Kuroiwa, M. Yamazawa, J. Akimitsu, K. Ohishi, A. Koda, W. Higemoto and R. Kadono., *Journal of the Physical Society of Japan* **74** 1386 (2005).

## FIGURE CAPTIONS

Fig. 1 X - ray diffraction patterns for nominal compositions  $(B/Nb) = 2.0, 2.1, 2.2, 2.3, 2.4$  and  $2.5$ .

Fig. 2 XPS spectra for nominal compositions  $(B/Nb) = 2.0, 2.1, 2.2, 2.3, 2.4$  and  $2.5$  before (a) and (b) after etching. The arrows indicate Nb, N, O, B states.

Fig. 3 XPS spectra Nb 3d of  $(B/Nb)_{XPS} = 2.00(6)$  before (a) and (b) after etching. The arrows indicate Nb states.

Fig. 4 XPS spectra Nb 3d in function of etching time for  $(B/Nb)_{XPS} = 2.00(6)$ . The arrows indicate Nb and boron states.

Fig. 5 XPS spectra for (a) Nb 3d and (b) B 1s for  $(B/Nb)_{XPS} = 2.00(6), 2.14(6), 2.15(6), 2.27(7), 2.31(7)$  and  $2.44(8)$  after etching. The open square line represents the experimental spectrum. The arrows indicate Nb and B states.

Fig. 6 Comparison of the measured  $(B/Nb)_{XPS} = 2.00(6)$  and  $2.44(8)$  Valence-Band with the total density of states (DOS) of  $NbB_2$  calculated in [15].

## TABLE CAPTIONS

Table 1. Positions of XPS spectral lines of B 1s, Nb 3d<sub>5/2</sub> and shift chemical in function of  $(B/Nb)_{XPS}$ .

Table 2. Densities of states at the Fermi level (states/eV atomic formula) [15].

FIGURE1

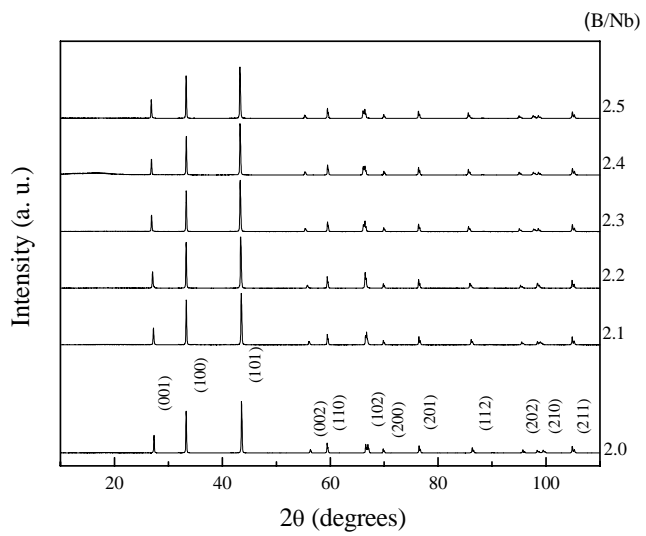


FIGURE2

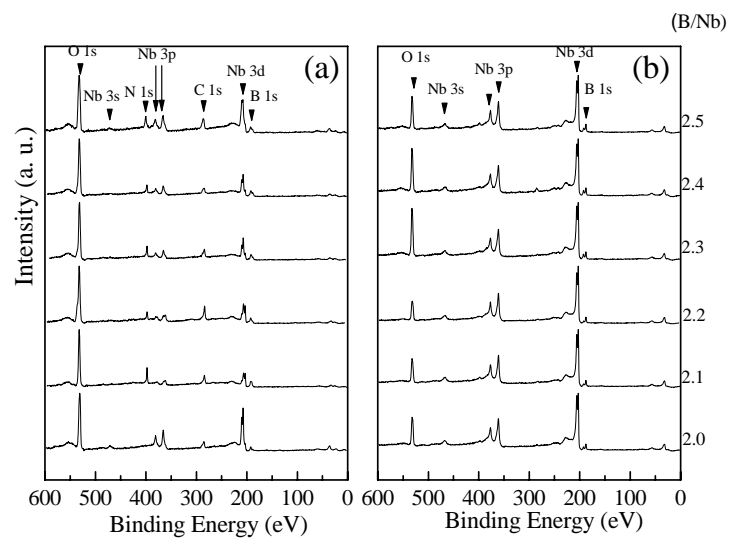


FIGURE3

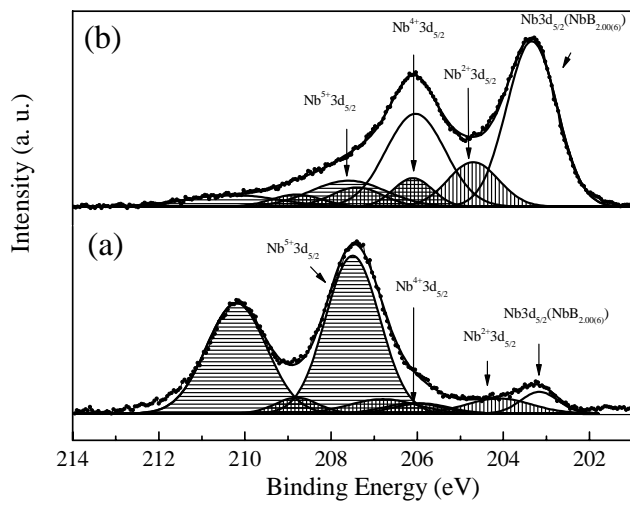


FIGURE4

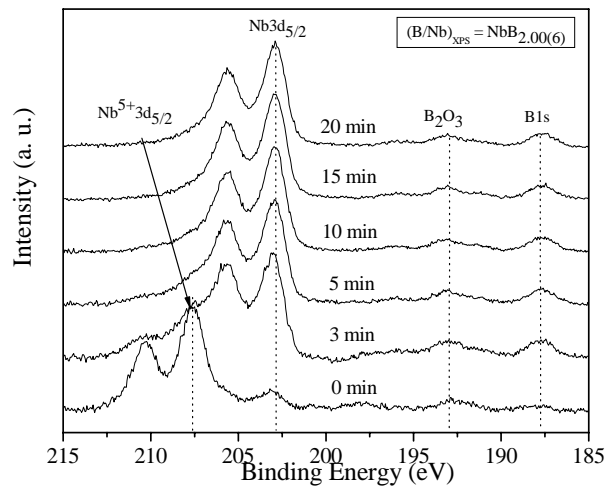


FIGURE5

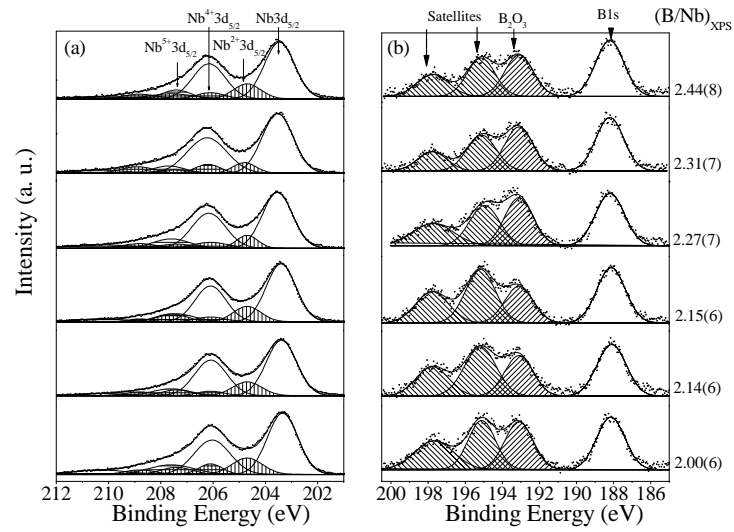


FIGURE6

